Journal of Hazardous Materials 217–218 (2012) 133–140

Contents lists available at SciVerse ScienceDirect

Journal of Hazardous Materials

journal homepage: www.elsevier.com/locate/jhazmat

Breakthrough analysis for water disinfection using silver nanoparticles coated resin beads in fixed-bed column

Nomcebo H. Mthombeni [a], Lizzy Mpenyana-Monyatsi [b], Maurice S. Onyango [a,*], Maggie N.B. Momba [b]

[a] Department of Chemical and Metallurgical Engineering, Tshwane University of Technology, Pretoria, South Africa
[b] Department of Environmental, Water and Earth Sciences, Tshwane University of Technology, Pretoria, South Africa

ARTICLE INFO

Article history:
Received 17 October 2011
Received in revised form 2 February 2012
Accepted 2 March 2012
Available online 7 March 2012

Keywords:
E. coli
Silver nanoparticles
Disinfection
Breakthrough analysis

ABSTRACT

This study demonstrates the use of silver nanoparticles coated resin beads in deactivating microbes in drinking water in a column filtration system. The coated resin beads are characterized using X-ray diffraction (XRD), Fourier transform infra-red (FT-IR), scanning electron microscope (SEM), transmission electron microscope (TEM) and energy dispersive spectroscopy (EDS) to confirm the functional groups, morphology and the presence of silver nanoparticles on the surface of the resin. The performance of the coated resin is evaluated as a function of bed mass, initial bacterial concentration and flow rate using *Escherichia coli* as model microbial contaminant in water. The survival curves of *E. coli* are expressed as breakthrough curves (BTCs), which are modeled using sigmoidal regression equations to obtain relevant rate parameters. The number of bed volumes processed at breakthrough point and capacity of the bed are used as performance indicators. Results show that performance increases with a decrease in initial bacterial concentration, an increase in flow rate and an increase in bed mass.

1. Introduction

Water-borne diseases are a direct indication of deterioration of water quality. The greatest water-borne risk to human health is microbial contamination of drinking water sources, leading to disease outbreaks [1]. It is estimated according to the WHO that 1.8 million people in the world die annually from diarrheal diseases (including cholera) of which 90% are children under 5, mostly in developing countries [2]. In terms of escalating demands and pollution of the limited water sources, particularly in rural and developing communities, the risk may even be relatively high [3].

To prevent or reduce the risk of waterborne diseases, many water utilities use disinfection processes. Chemical and physical processes such as chlorination [4], ultraviolet light [5,6], reverse osmosis and use of silver catalyst [7] are well developed. However, these disinfection processes raise health, economic or technical issues. For instance, chemical disinfectants such as free chlorine, chloramines and ozone can react with various constituents in natural water to form disinfection byproducts which are harmful to health. Studies have also shown that resistance of pathogens such as *Cryptosporidium* and *Giardia*, to conventional chemical disinfection implies that a large dosage of chemicals is required [8]. Other methods like UV purification and reverse osmosis are not cost effective [9]. Because of the limitations of the conventional methods there is a need to explore other innovative alternatives such as the use of nanotechnology.

Nanotechnology is considered as a new generation of technology, is revolutionary and will impact on economies through new consumer products, manufacturing methods and materials usage [10]. The technology could lead to cost effective and high performance water treatment systems [11]. Under this new technology, the use of oligodynamic nanoparticles for water disinfection is being explored. Oligodynamic nanoparticles based disinfection includes the use of metals such as silver, gold, zinc, tin and copper due to their antimicrobial properties. Besides their oligodynamic nature, they also possess catalytic properties [12]. Ever since silver was recognized as a biocide, its application in purification of water is increasing. In nanoparticle form, silver becomes more reactive, has increased catalytic properties, large surface area to volume ratio, unusual crystal morphologies and thus toxic than silver ion [13,14]. To effectively apply silver nanoparticles in water disinfection, they should be impregnated in a substrate.

Several studies have shown the use of silver nanoparticles coated on various substrates. For instance, silver nanoparticles were incorporated in materials such as montmorillonites [15], polysulfone [16] cellulose acetate [17], fiberglass [18], polyurethane foams [19], ceramic filters [20], activated carbon [21,22]. There is however concerns about the ability of carbon based substrates to completely remove bacteria because it has been

* Corresponding author at: Private Bag X680, Pretoria 0001, Staatsartillerie Road, Pretoria West, South Africa. Tel.: +27 12 3823533; fax: +27 12 3823532.
E-mail addresses: OnyangoMS@tut.ac.za, onyi72uk@yahoo.co.uk (M.S. Onyango).

0304-3894/$ – see front matter © 2012 Elsevier B.V. All rights reserved.
doi:10.1016/j.jhazmat.2012.03.004

reported that bacteria metabolize carbon [23], and that bacteria attached to carbon can be a source of contamination of water in treated water supplies [24]. Moreover, most of the above studies were inclined towards testing antibacterial properties of the prepared media using the plate culture technique but failed to consider detailed breakthrough analysis that can aid water treatment systems design. In addition, silver nanoparticles loaded on some of the above substrates/media showed poor disinfection performance and are not structurally stable for use in water treatment systems. Thus there still exists a need to explore nanotechnology-based water disinfection in appropriate system configuration such as fixed-bed. Water treatment using fixed beds has inherent advantages such as production of high quality drinking water, its simplicity, ease of operation and handling, and being suitable for use as a point-of-use (POU) system [25]. The foregoing discussion warranties the need to search for alternative substrates that show good disinfection performance, are structurally stable and hydraulically conducive to perform transport experiments in fixed beds.

Consequently, in this study polystyrene resin beads were coated with silver nanoparticles and were applied in deactivating *Escherichia coli* as model biological contaminant in water. Immobilization of metal nanoparticles on the surface of polystyrene beads is one of the most popular routes for their synthesis [26], and the entrapment of silver nanoparticles is due to electrostatic attraction between polystyrene beads and the oppositely charged complex precursor ions [27]. The silver nanoparticles coated resin was then used to perform breakthrough analysis. To the best of our knowledge there is very little information in literature on breakthrough analysis using silver nanoparticles in fixed bed column for water disinfection. Yet, for system design to achieve optimal operation of water disinfection systems, breakthrough data and modeling are prerequisite. It is for these reasons that the fixed-bed performance was investigated under various process conditions; namely, flow rate, initial bacterial concentration and bed mass for the effective inactivation of *E. coli*. Empirical models were utilized to tract parameters for the analysis of breakthrough curves in the fixed bed column. Furthermore, the number of bed volumes processed and the antibacterial media exhaustion rate were used as performance indicators.

2. Materials and methods

2.1. Materials

Rohm and Haas Amberlite-IR-120 (hydrogen form) cation resin used in the study was purchased from Lenntech (Johannesburg, South Africa). Silver nitrate and reducing agent sodium borohydride was purchased from Merck (South Africa). Nutrient broth and agar were also purchased from Merck. The microbial strain used for the inactivation experiments was *E. coli* (ATCC 43895), from the American Type Culture Collection.

2.2. Preparation of silver nanoparticle coated resin beads

Silver was coated on the cation resin beads by modifying the method described by Nath et al. [28] to obtain optimum conditions for deactivating *E. coli*. Accordingly, liquid ammonia (25%) was added to 200 mL aqueous solution of 0.1 M $AgNO_3$. Then a known amount (20 g) of cation exchange resin was mixed with the silver amine complex and stirred using a magnetic stirrer for 3 h. Afterwards, the resin coated with silver amine was washed three times with distilled water and heated in an oven at 150 °C for 1 h. Then freshly prepared aqueous solution of 0.01 M sodium borohydride was used to reduce the silver oxide-resin beads to zero-valent silver nanoparticles. The resulting silver nanoparticle coated resin beads were washed three times with distilled water and dried in a water bath at 65 °C overnight. Finally, the dry silver nanoparticles coated resin beads were used for characterization and microbial inactivation tests.

2.3. Characterization

The structure of the resin beads was characterized by using an ALPHA Fourier transformed infra-red (FT-IR) spectrometer (Bruker Optics GmbH, Ettlingen, Germany), on the attenuated total reflection (ATR) diamond crystal at 4 cm^{-1} resolution. Surface morphology of the silver nanoparticles coated on the resin substrate was examined with a JSM-5800LV JEOL (JEOL Ltd, Tokyo, Japan) scanning electron microscope (SEM) coupled with X-ray energy dispersive spectroscopy (EDS). The EDS using a NanoTrace detector (Thermo Fisher Scientific, Inc.) at an accelerating voltage of 20 kV was applied to confirm the silver content on the substrate. JEOL 2100F (JEOL Ltd, Tokyo, Japan) transmission electron microscope (TEM) with an electron beam operating at 100 kV was used to examine the size of the silver nanoparticles coated on the resin beads. The TEM samples were prepared by dispersing a drop of the colloid on a copper grid, which was coated with a carbon film to reduce charging. X-ray diffraction (XRD) measurement was performed on a Bruker D8 Advance (Cu Kα, radiation with 1.5416 Å wavelengths) diffractometer.

2.4. Fixed bed column experiments

E. coli (ATCC 43895) was selected as a model biological contaminant in water. Column experiments were performed using a polyvinyl chloride (PVC) column of 20 mm diameter and 30 cm length. Each column was packed with resin beads coated with silver nanoparticles with glass beads and glass wool placed in the upper and bottom ends of each column to hold the disinfection media. The column was washed and sterilized under UV light for 30 min. The glass beads and wool were autoclaved before use. Water contaminated with *E. coli* was pumped vertically upwards continuously through the column using a Rainin Dynamax peristaltic pump. The effect of several process variables was explored as described below.

2.4.1. Effect of bed mass of antibacterial material

Contaminated water containing *E. coli* bacterial strain at initial concentration of 6×10^3 CFU/mL was pumped through column at different mass of 5, 10, 15 and 20 g of silver nanoparticles coated cation resin beads, at a flow rate of 2 mL/min. The effluent samples were collected at 60 min time intervals and analyzed for viable cells using spread plate technique.

2.4.2. Effect of flow rate

Bacterial contaminated water at initial concentration of 6×10^3 CFU/mL of *E. coli* was pumped vertically upward at a flow rate of 2, 5, 7 and 10 mL/min through columns packed with 15 g silver nanoparticles coated resin beads. Effluent collection and viable cells analysis was done as in Section 2.4.1.

2.4.3. Effect of initial concentration

The mass of silver coated resin material was kept constant at 15 g while contaminated water was pumped at a constant flow rate of 2 mL/min through the column. The initial concentrations of *E. coli* were 6.5×10^4, 1.6×10^4, 6×10^3 and 6.6×10^2 CFU/mL. Effluent collection and viable cells analysis was done as in Section 2.4.1.

2.4.4. E. coli removal from environmental water

Two environmental water samples (groundwater) were collected from Delmas boreholes in Mpumalanga Province of South

Africa. In the dynamic experiments, the water was pumped vertically upward at a flow rate of 2 mL/min through columns packed with 15 g silver nanoparticles coated resin beads. Effluent collection and viable cells analysis was done as in Section 2.4.1.

2.5. Enumeration of viable cells

Samples from the effluent were collected in sterile conical flasks at known time intervals of 60 min. The collected samples were neutralized by adding 1 mL of 15% sodium thiosulfate. Effluent samples were analyzed for bacterial concentration. The bacterial concentration was determined by serial diluting in sterile saline solution and plated on selective medium by using spread plate technique according to Standard Methods [29]. Triplicate plates were used for counting viable cells from each diluted suspension and average values used. Inactivation data are expressed as N_t/N_i, with N_t being survivor colonies at any time and N_i being the bacterial load in the column influent.

2.6. Modeling of breakthrough curves using non-linear equations

Non-linear sigmoidal regression models are utilized to fit and extract model parameters. When N_i cells of *E. coli* are filtered through the column bed containing resin modified with Ag nanoparticles, a series of N_t survivor colonies are obtained at time intervals t. A plot of N_t versus t generates a sigmoidal curve. Empirical sigmoidal models utilized in this study are: logistic, Gompertz and Boltzmann equations.

The general form of the logistic equation used to analyze breakthrough data is:

$$N_t = \frac{N_i}{1 + e^{-k(t-t_{50})}} \tag{1}$$

which resolves to

$$ln\left(\frac{N_t}{N_i - N_t}\right) = k(t - t_{50}) \tag{2}$$

where k (min^{-1}) is the rate constant which is a measure of the steepness of the slope of the breakthrough curves. The time it takes to reach median concentration (half N_i) of bacterial count is referred to as t_{50} (min). The Gompertz equation is given as:

$$N_t = N_i e^{-\exp(-k(t-t_{50}))} \tag{3}$$

The linear form of Eq. (3) is given by:

$$\ln \ln \frac{N_t}{N_i} = -k(t - t_{50}) \tag{4}$$

where t_{50} is the center at inflection point, N_i/e. The Boltzmann sigmoidal regression equation takes the form:

$$N_t = \frac{N_i - N_o}{1 + e^{((t-t_{50})/k)}} + N_0 \tag{5}$$

where N_o is the bottom asymptote, which is the bed bacterial concentration at time zero. In this study the value of N_o is considered to be zero, and t_{50} in the Boltzmann equation is $[(N_i + N_o)/2]$. Therefore Eq. (5) reduces to:

$$N_t = \frac{N_i}{1 + e^{((t-t_{50})/k)}} \tag{6}$$

which linearizes to

$$ln\frac{N_t}{N_i} = \frac{1}{k}(t - t_{50}) \tag{7}$$

The models described in Eqs. (1)–(7) were fitted to the experimental data using Origin 6.0 software and the extracted parameters are summarized in Table 1.

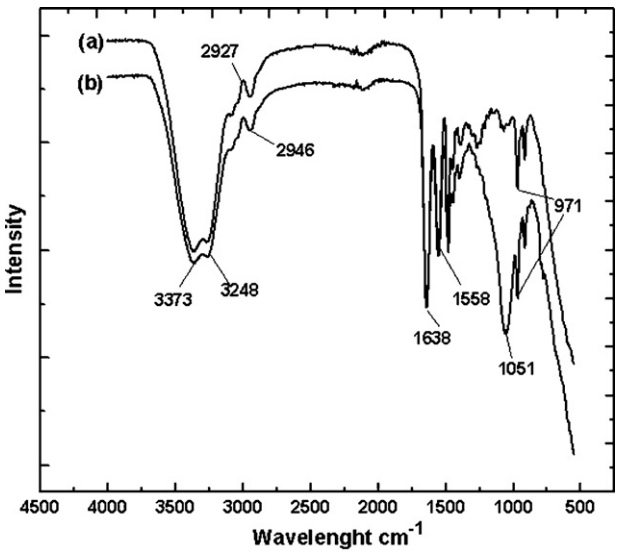

Fig. 1. FT-IR spectra of resin beads before coating (a) and resin coated with silver nanoparticle (b).

When operating a fixed bed column, the objective is to reduce the concentration of a given contaminant to a value below the maximum allowable concentration. For a given bed mass the performance is directly related to the number of bed volumes processed before the breakthrough point (point when *E. coli* is first detected column effluent) is reached. The number of bed volumes is given by the following equation:

$$\text{BV} = \frac{\text{Volume of water at breakthrough point(L)}}{\text{Volume of antibacterial material bed(L)}} \tag{8}$$

The rate of at which the antibacterial material become exhausted indicates how often the material is replaced and the operating costs involved. The antibacterial material exhaustion rate (AER) is defined as the mass of antibacterial material exhausted per volume of water treated at breakthrough point and is expressed as:

$$\text{AER} = \frac{\text{Mass of antibacterial material(g)}}{\text{Volume of water treated(L)}} \tag{9}$$

Low value of AER indicates good performance of the bed and is the main performance indicator for comparing different operating conditions.

3. Results and discussion

3.1. Characterization

The FT-IR spectra shown in Fig. 1 are used to identify the functional groups present on the resin beads. The FT-IR spectrum of resin beads before coating with silver (Fig. 1(a)) depicts peaks at 3373, 3248, 2927 cm^{-1} that are considered to arise from the O—H stretching vibration of carboxylic, while the C=C stretching vibration of aromatic, the N—H bend mode of C—NH_3^+ and the S—O stretching vibration of sulfonates are observed at 1638, 1558, and 971 cm^{-1}, respectively. Similar peaks corresponding to the functional groups were also confirmed by Smith [30] and Özacar et al. [31]. The O—H vibration shifted by 19 cm^{-1} from 2927 cm^{-1} to 2946 cm^{-1} after coating the resin with silver-nanoparticles indicating the interaction of silver nanoparticles with the resin beads (Fig. 1(b)).

Elemental composition and morphology of resin coated with silver nanoparticles were investigated by scanning electron microscopy (SEM) assisted with energy dispersive X-ray spectroscopy analysis (EDS). Fig. 2 shows the SEM image of a silver

Table 1
Summary of model parameters for water disinfection using silver nanoparticle coated resin beads in fixed bed column.

	Logistic model parameters			Gompertz model parameters			Boltzmann model parameters		
	Rate constant k (min^{-1})	Time at $N_i/2$ t_{50} (min)	R^2	Rate constant k (min^{-1})	Time at N_i/e t_{50} (min)	R^2	Rate constant k (min^{-1})	Time at $N_i/2$ t_{50} (min)	R^2
Mass of antibacterial material (g)									
5	0.00426	1325	0.978	0.00189	1283	0.968	0.00426	1325	0.978
10	0.00527	2841	0.979	0.00201	2927	0.979	0.00527	2841	0.979
15	0.00577	4373	0.996	0.00256	4362	0.993	0.00577	4373	0.996
20	0.00696	6048	0.990	0.00262	6126	0.994	0.00696	6048	0.990
Flow rate (mL/min)									
2	0.00577	4373	0.996	0.00256	4362	0.993	0.00577	4373	0.996
5	0.01718	3110	0.993	0.01116	3077	0.994	0.01718	3110	0.993
7	0.01353	2705	0.994	0.00787	2668	0.993	0.01353	2705	0.994
10	0.01212	2442	0.988	0.00588	2434	0.983	0.01212	2442	0.988
Initial bacterial concentration (CFU/mL)									
660	0.00823	5389	0.988	0.00485	5330	0.991	0.00823	5389	0.988
6000	0.00577	4373	0.996	0.00256	4362	0.993	0.00577	4373	0.996
16000	0.01007	2479	0.986	0.00535	2432	0.985	0.01007	2479	0.986
65000	0.07317	1774	0.991	0.04717	1760	0.989	0.07317	1774	0.991
Environmental water									
A4	0.00485	11286	0.995	0.00291	11180	0.997	0.00485	11286	0.995
A7	0.023	9078	0.979	0.01695	9055	0.973	0.023	9078	0.979

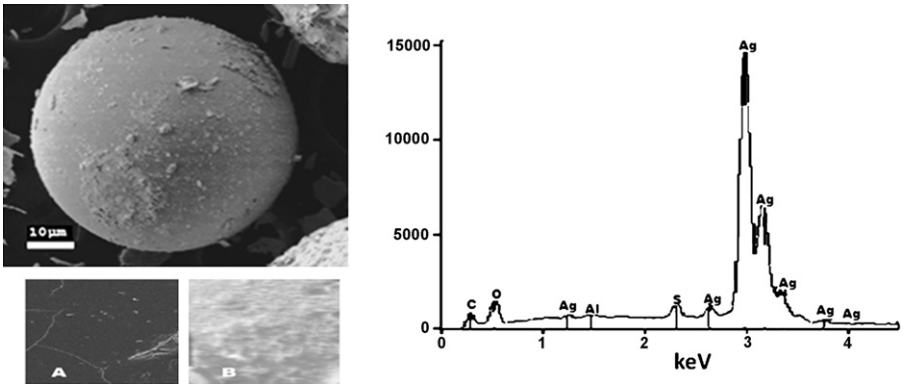

Fig. 2. SEM image (left) and EDS spectra of silver coated resin bead. The insert on the SEM image shows surface of resin bead before coating (A) and a coated film on the surface of the resin bead (B).

nanoparticles-coated resin bead, indicating the complete coverage of polystyrene beads with silver. The inserted images show the silver free resin surface (A) and as can be observed silver formed a thin layer (B) on the surface of the resin after synthesis. The EDS spectra confirm the presence of metallic silver on the resin particles. The TEM image (Fig. 3) of the coated resin bead confirms that the silver is indeed nano-scale in size. Specifically, the silver nanoparticles are within a size range of 15–50 nm. The diffraction pattern of the synthesized silver nanoparticles on cation resin beads shown in Fig. 4 matches the face-centered cubic (fcc) structure of silver observed at 2θ angle 37.7°, 44.0°, 64.2° and 77.1°. These correspond to the four diffraction peaks (1 1 1), (2 0 0), (2 2 0) and (3 1 1) crystal planes, respectively, indicating the formation of metallic silver nanoparticles on the surface of the cation resin beads.

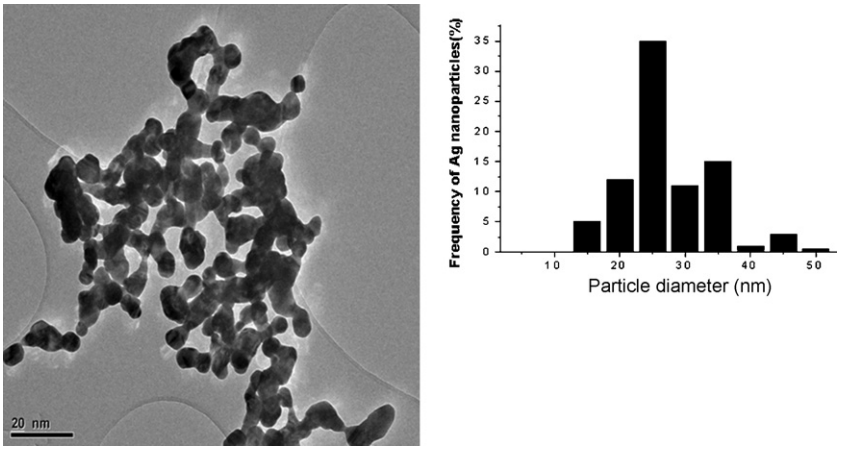

Fig. 3. Histogram of size distribution of silver nanoparticles. The inserted figure shows the TEM image of silver nanoparticles coated on resin beads.

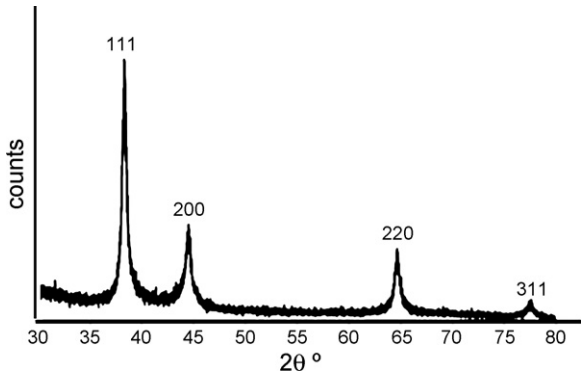

Fig. 4. XRD patterns of the silver nanoparticles coated on cation resin.

3.2. Breakthrough analysis for water disinfection

Operating parameters such as bed mass, flow rate and initial bacterial loading are very important when designing a column for water treatment. In this study the effects of these parameters for water disinfection by resin beads coated with silver nanoparticles were investigated.

3.2.1. Effect of mass of antibacterial material

By varying the bed mass of the resin media coated with silver nanoparticles and fixing the flow rate and initial bacterial loading in the influent, the amount of active sites in the material available and the contact time between bacteria and the antibacterial material are increased. In this experimental run, the initial *E. coli* concentration was 6×10^3 and the flow rate was set at 2 mL/min. The effect of variation of bed mass is shown in Fig. 5 as breakthrough curves (BTCs). As can be seen, the predicted and experimental breakthrough curves compare very well for all the three sigmoidal models. From the BTCs, the various model parameters were determined and are summarized in Table 1. The parameters k and t_{50} increase with an increase in the mass of the antibacterial material. The trend in k and t_{50} may be explained by the fact that as the mass is increased, there are more active silver sites present to inactivate the bacteria. Silver is required to attach, accumulate and penetrate the inside of the bacterial membrane to inactivate and cause cell malfunction [32–34]. Meanwhile, the volumes processed at breakthrough point (when 1 CFU/mL was present in the column effluent) were 1.8, 3.6, 7.2 and 11.16 for 5, 10, 15 and 20 g bed masses, respectively. The corresponding bed volumes (BVs) are 94, 133, 216 and 273 and the AER values are 2.8, 2.1 and 1.8 g/L for 5, 10, 15 and 20 g, respectively. The lower the AER value the better the performance of the column. The results indicate that it is favorable to increase the bed mass as it increases the bed performance in inactivating microorganisms. The increased performance can be attributed to the fact that the contact time between the *E. coli* bacteria and active media increases resulting in increased inactivation performance.

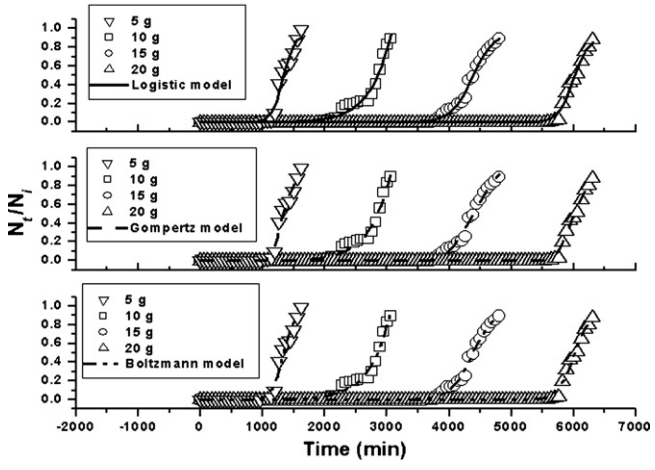

Fig. 5. Breakthrough curves for the removal of *E. coli* from water using silver nanoparticles coated resin beads at different bed masses. Initial bacterial concentration = 6000 CFU/mL and flow rate = 2 mL/min.

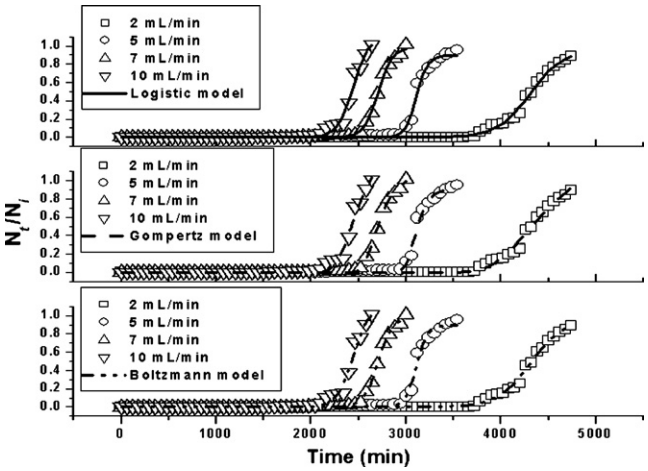

Fig. 6. Breakthrough curves for the removal of *E. coli* from water using silver nanoparticles coated resin beads at different flow rates. Initial bacterial concentration = 6000 CFU/mL, antibacterial material mass = 15 g.

3.2.2. Effect of flow rate

Contaminated water was pumped in an upward flow mode at an average volumetric flow rate of 2, 5,7 and 10 mL/min while the bed mass and initial *E. coli* concentration were maintained at 15 g and 6×10^3 CFU/mL, respectively. The results are summarized in Fig. 6 in which it is shown that more processing time was required for low flow rate for breakthrough to be reached. For all the three sigmoidal models, the experimental and predicted curves match very well. As expected, all the models predict a decrease in t_{50} parameter as the flow is increased. There is no specific trend in the values of k. The volume processed at breakthrough point was found to be 7.2, 10.2, 12.6 and 14.4 with corresponding bed volumes of 218, 309, 382 and 436 for 2, 5, 7 and 10 mL/min, respectively. The AER values obtained are 2.1, 1.4, 1.2 and 1.0 g/L (see Table 2) at the flow rate of 2, 5, 7, and 10 mL/min, respectively. The effect of flow rate on the bacterial inactivation can be due to various factors, such as, the mechanical stress promoted by the movement of the water in which bacteria are dispersed and the contact time of bacteria with the antibacterial material bed [34].

3.2.3. Effect of initial concentration

The bacterial concentration in contaminated water can have a very wide range of variation depending on the nature of the source water. As such it is important to know how a given media will perform under such conditions. Consequently, the influent contaminated water at three different initial concentrations of 6.6×10^2, 6×10^3, 1.6×10^4 and 65×10^4 CFU/mL were used in the study while a bed mass of 15 g and a flow rate of 2 mL/min was maintained throughout the experimental run. The BTC obtained from the investigation of the effect of initial bacterial concentration is shown in Fig. 7. The experimental and predicted curves match very well. It is observed that the breakthrough point decreases with an increase in initial bacterial concentration. As a result, all the models predict a decrease in t_{50} parameter as the initial concentration of bacteria

Table 2
Summary of results at breakthrough point.

	Time at breakthrough point t_b (min)	Capacity (CFU/g)	Volumes processed at breakthrough (L)	Bed volume processed (L)	AER (g/L)
Mass of antibacterial material (g)					
5	960	2.09×10^6	1.80	94	2.8
10	1800	2.16×10^6	3.60	133	2.8
15	3600	2.90×10^6	7.20	218	2.1
20	5580	3.34×10^6	11.2	273	1.8
Flow rate (mL/min)					
2	3600	2.90×10^6	7.20	218	2.1
5	2040	4.08×10^6	10.2	309	1.4
7	1800	5.04×10^6	12.6	382	1.2
10	1440	5.70×10^6	14.4	436	1.0
Initial bacterial concentration (CFU/mL)					
660	4740	4.16×10^5	9.50	283	1.6
6000	3600	2.9×10^6	7.20	216	2.1
16000	2220	4.44×10^6	4.50	133	3.4
65000	540	7.15×10^7	1.10	33	13.6
Environmental water					
A4	10680	1.17×10^5	21.4	647	0.70
A7	8768	1.73×10^5	17.5	531	0.86

increases. This is due to the fact that at higher bacterial concentration, more silver is required to effect bacteria inactivation. Because quantity of the inactivation media is fixed, the breakthrough point and t_{50} are reached faster. There is no specific trend in the values of k. The volumes of water treated at breakthrough point were 9.4, 7.2, 4.44 and 1.1, and the corresponding BV are 283, 216,133 and 33 at the initial bacterial concentration of 6.6×10^2, 6×10^3, 1.6×10^4 and 65×10^4 CFU/mL, respectively. More bacterial cells are inactivated at higher initial bacterial concentration as indicated by capacity values (CFU/g) in Table 2. This effect can be due to the fact that an increased initial bacterial cell loading (i) enhances the probability of interaction between bacterial cells and the silver nanoparticles (ii) reduces the overall mass transfer limitations and (ii) results in an increase in inactivation rate [35,36]. The AER values obtained are 1.6, 2.1, 3.4 and 13.6 for 6.6×10^2, 6.0×10^3 and 1.6×10^4, respectively. High values of AER at higher initial bacterial concentration indicate that in operation the coated resins will need to be replaced at a higher frequency when processing water containing higher initial cells concentration.

3.2.4. *E. coli* removal from environmental water

Two borehole water samples coded A4 and A7 with *E. coli* concentrations of 85 and 150 CFU/mL, respectively, were used to explore the capability of silver nanoparticles coated resin beads to disinfect real water. The physico-chemical characteristics of the borehole water samples used in this study are summarized in Table 3. Most of the water quality parameters are within the acceptable limit as defined by the South African National Standards (SANS241). The BTCs for the two borehole water samples are shown in Fig. 8. An earlier breakthrough point is observed for sample A7 which agrees with results presented in Section 3.2.3 in which higher concentration was found to lead to a faster saturation of the bed. Meanwhile the experimental and predicted BTCs match very well. A summary of the three models parameters is given in Table 1. All the models predict a higher value of t_{50} for sample A4 which had a lower *E. coli* concentration. The volumes of water treated at breakthrough point were 21.4 and 17.5 and the corresponding BV are 647 and 531 for samples A4 and A7, respectively. More bacterial cells are inactivated for sample A7 compared to sample A4 as indicated by capacity values (CFU/g) in Table 2. This observation is due to the fact that sample A7 had a higher initial concentration of bacterial cells. The computed AER values are 0.70 and 0.86 for sample A4 and A7, respectively. As such the frequency of exhaustion and replacement of the media will be faster when processing sample A7 in comparison to sample A4.

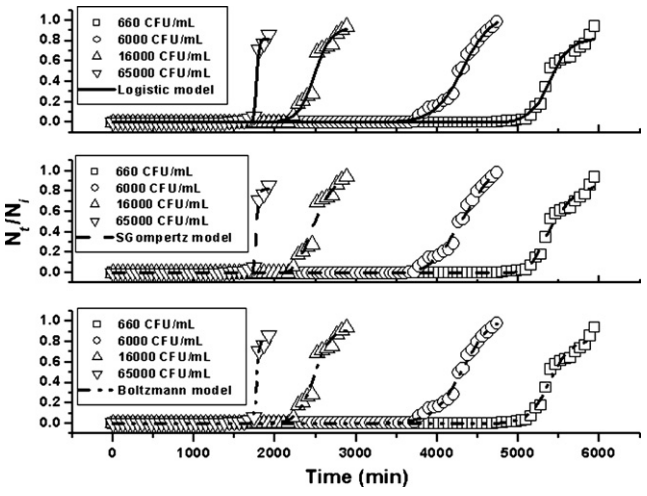

Fig. 7. Breakthrough curves for the removal of *E. coli* from water by silver nanoparticles coated resin beads at different initial bacterial concentrations. Flow rate = 2 mL/min, mass of antibacterial material = 15 g.

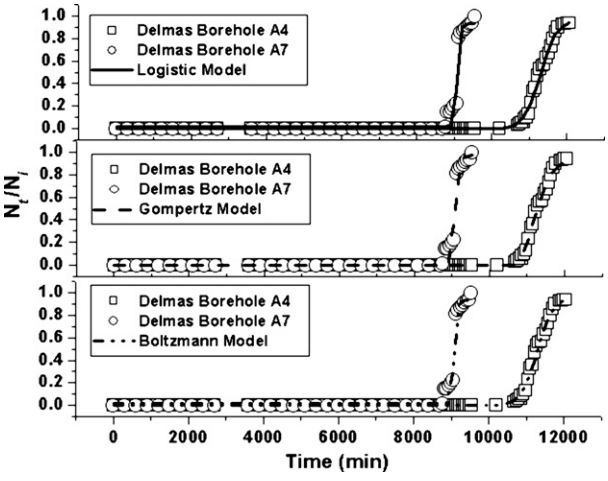

Fig. 8. Breakthrough curves for the removal of *E. coli* from environmental water. Sample A4 initial bacterial concentration = 85 CFU/mL, sample A7 initial bacterial concentration = 150 CFU/mL, flow rate = 2 mL/min, mass of antibacterial material = 15 g.

Table 3
Selected physico-chemical property of raw water from Delmas Boreholes (A4 and A7).

Parameters	Units	A4	A7	SANS 241
Escherichia coli	CFU/mL	85	150	<1
pH		8.94 ± 0.61	7.22 ± 0.14	5.0–9.5
Turbidity	NTU	2.78 ± 0.96	1.59 ± 0.11	<1
Fluorides	mg/L	41.21 ± 0.92	0.46 ± 0.18	<1
Nitrates	mg/L as N	14.16 ± 1.13	1.59 ± 0.02	<10
Calcium	mg/L as Ca	126.89 ± 4.52	98.25 ± 1.12	<150
Magnesium	mg/L as Mg	62.87 ± 0.31	26.36 ± 7.18	<70
Phosphates	mg/L	18.14 ± 3.79	1.00 ± 0.04	
Arsenic	mg/L	7.49 ± 2.58	2.99 ± 0.12	<10 μg/L
Iron	mg/L	0.40 ± 0.18	0.40 ± 0.18	<200 μg/L

4. Conclusions

E. coli inactivation was investigated using resin beads modified with silver nanoparticles in a column experimental set up. Results showed that the breakthrough point where bacteria first appeared in the effluent water was reached faster at lower bed mass, higher bacterial concentration and high flow rate. Three sigmoidal models were successfully used to interpret the breakthrough curves. The AER and the number of BVs processed at breakthrough point were used as performance indicators. Low values of AER and large BV were observed at lower bacterial concentration, higher flow rate and higher bed mass. This study has shown that nanoparticles coated resins can be used to inactivate bacteria and be employed in water treatment. Concentrations of bacteria used are typically higher than those that would be found in environmental water and as preliminary results suggest, the material is expected to perform extremely well when treating environmental water of low bacterial cell concentration.

Acknowledgment

The authors acknowledge the National Research Fund (NRF)-South Africa for the financial support provided under the National Nanotechnology Flagship Programme.

References

[1] World Health Organisation, Guidelines for Drinking Water Quality, third ed., USA, 2004.
[2] World Health Organisation, Water, sanitation and hygiene links to health. Facts and figures, 2004.
[3] W.O.K. Grabow, Waterborne diseases: update on water quality assessment and control, Water SA 22 (1996) 193–202.
[4] H. Son, M. Cho, J. Kim, B. Oh, H. Chung, J. Yoon, Enhanced disinfection efficiency of mechanically mixed oxidants with free chlorine, Water Res. 39 (2005) 721–727.
[5] G. Finch, E. Black, L. Gyurek, Ozone and chlorine inactivation of Cryptosporidium, in: Water Quality Technology Conference, AWWA, 1994, pp. 1303–1309.
[6] W. Gujer, U. von Gunten, A stochastic model of an ozonation reactor, Water Res. 37 (2003) 1667–1677.
[7] E. Hassinger, A.D. Thomas, B.B. Paul, Reverse Osmosis Units Water Facts, 1994.
[8] V. Shashikala, V. Siva Kumar, A.H. Padmasri, B. David Raju, S. Venkata Mohan, P. Nageswara Sarma, K.S. Rama Rao, Advantages of nano-silver-carbon covered alumina catalyst prepared by electro-chemical method for drinking water purification, J. Mol. Catal. A – Chem. 268 (2007) 95–100.
[9] Q. Li, S. Mahendra, D.Y. Lyon, L. Brunet, V.L. Michael, D. Li, P.J.J. Alvarez, Antimicrobial nanomaterials for water disinfection and microbial control: potential applications and implications, Water Res. 42 (2008) 4591–4602.
[10] M.A. Albrecht, C.W. Evans, C.L. Raston, Green chemistry and the health implications of nanoparticles, R. Soc. Chem. 8 (2006) 417–432.
[11] M.S. Diallo, N. Savage, Nanoparticles and water quality, Nanopart. Res. 7 (2005) 325–330.
[12] I. Rodríguez Iznaga, V. Petranovskii, G. Rodríguez Fuentes, C. Mendoza, A. Benítez Aguilar, Exchange and reduction of Cu^{2+} ions in clinoptilolite, J. Colloid Interface Sci. 316 (2007) 877–886.
[13] O. Choi, K.K. Deng, N.J. Kim, L. Ross Jr., R.Y. Surampalli, Z. Hu, The inhibitory effects of silver nanoparticles, silver ions, and silver chloride colloids on microbial growth, Water Res. 4 (2) (2008) 3066–3074.
[14] G. Ren, D. Hu, E.W.C. Cheng, M.A. Vargas-Reus, P. Reip, R.P. Allaker, Characterisation of copper oxide nanoparticles for antimicrobial applications, Int. J. Antimicrob. Agents 33 (2009) 587–590.
[15] S.M. Magaña, P. Quintana, D.H. Aguilar, J.A. Toledo, C. Ángeles-Chávez, M.A. Cortés, L. León, Y. Freile-Pelegrín, T. López, R.M.T. Sánchez, Antibacterial activity of montmorillonites modified with silver, J. Mol. Catal. A – Chem. 281 (2008) 192–199.
[16] K. Zodrow, L. Brunet, S. Mahendra, D. Li, A. Zhang, Q. Li, P.J.J. Alvarez, Polysulfone ultrafiltration membranes impregnated with silver nanoparticles show improved biofouling resistance and virus removal, Water Res. 43 (2009) 715–723.
[17] W. Chou, D. Yu, M. Yang, The preparation and characterization of silver-loading cellulose acetate hollow fiber membrane for water treatment, Polym. Adv. Technol. 16 (8) (2005) 600–607.
[18] G. Nangmenyi, Z. Yue, S. Mehrabi, E. Mintz, J. Economy, Synthesis and characterization of silver-nanoparticle-impregnated fiberglass and utility in water disinfection, Nanotechnology 20 (2009).
[19] P. Jain, T. Pradeep, Potential of silver nanoparticle-coated polyurethane foam as an antibacterial water filter, Biotechnol. Bioeng. 90 (2005) 59–63.
[20] V. Oyanedel-Craver, J. Smith, Sustainable colloidal-silver-impregnated ceramic filter for point-of-use water treatment, Environ. Sci. Technol. 42 (3) (2008) 927–933.
[21] K.Y. Yoon, J.H. Byeon, C.W. Park, J. Hwang, Antimicrobial effect of silver particles on bacterial contamination of activated carbon fibers, Environ. Sci. Technol. 42 (4) (2008) 1251–1255.
[22] S. Zhang, R. Fu, D. Wu, W. Xu, Q. Ye, Z. Chen, Preparation and characterization of antibacterial silver-dispersed activated carbon aerogels, Carbon 42 (2004) 3209–3216.
[23] M.H. Saier, Multiple mechanisms controlling carbon metabolism in bacteria, Biotechnol. Bioeng. 58 (1998) 170–174.
[24] A.K. Camper, M.W. LeChevallier, S.C. Broadaway, G.A. McFeters, Bacteria associated with granular activated carbon particles in drinking water, Appl. Environ. Microbiol. 52 (1986) 434–438.
[25] M.S. Onyango, T.Y. Leswifi, O. Aoyi, D. Kuchar, F.A.O. Otieno, H. Matsuda, Breakthrough analysis for water defluoridation using surfactant-tailored zeolite fixed-bed column, Ind. Eng. Chem. Res. 48 (2009) 931–939.
[26] P.A. Schueler, J.T. Ives, F. DeLaCroix, W.B. Lacy, P.A. Becker, J. Li, K.D. Caldwell, B. Drake, J.M. Harris, Physical structure, optical resonance, and surface-enhanced Raman scattering of silver-island films on suspended polymer latex particles, Anal. Chem. 6 (5) (1993) 3177–3186.
[27] S. Jana, S.K. Ghosh, S. Nath, S. Pande, S. Praharaj, S. Panigrahi, S. Basu, T. Endo, T. Pal, Synthesis of silver nanoshell-coated cationic polystyrene beads: a solid phase catalyst for the reduction of 4-nitrophenol, Appl. Catal. A – Gen. 313 (2006) 41–48.
[28] S. Nath, S.K. Ghosh, S. Kundu, S. Praharaj, S. Panigrahi, S. Basu, T. Pal, A convenient approach to synthesize silver nanoshell covered functionalized polystyrene beads: a substrate for surface enhanced Raman scattering, Mater. Lett. 59 (2005) 3986–3989.
[29] APHA, Standard Methods for the Examination of Water and Wastewater, AWWA, and Water Pollut. Control Fed., Washington, DC, 1998.
[30] B. Smith, Infrared Spectral Interpretation: A Systematic Approach, CRC Press, USA, 1999.
[31] M. Özacar, I.A. Sengil, H. Türkmenler, Equilibrium and kinetic data, and adsorption mechanism for adsorption of lead onto valonia tannin resin, Chem. Eng. J. 143 (2008) 32–42.
[32] J.R. Morones, J.L. Elechiguerra, A. Camacho, K. Holt, J.B. Kouri, J.T. Ramirez, M.J. Yacaman, The bactericidal effect of silver nanoparticles, Nanotechnology 16 (2005) 2346–2353.
[33] I. Sondi, B. Salopek-Sondi, Silver nanoparticles as antimicrobial agent: a case study on *E. coli* as a model for gram-negative bacteria, J. Colloid Interface Sci. 275 (2004) 177–182.

[34] A.I. Gomes, J.C. Santos, V.J.P. Vilar, R.A.R. Boaventura, Inactivation of Bacteria *E. coli* and photodegradation of humic acids using natural sunlight, Appl. Catal. B – Environ. 88 (2009) 283–291.
[35] P.S.M. Dunlop, J.A. Byrne, N. Manga, B.R. Eggins, The photocatalytic removal of bacterial pollutants from drinking water, Photochem. Photobiol. A – Chem. 148 (2002) 355–363.
[36] M.N. Chonga, B. Jina, H. Zhu, C. Saint, Bacterial inactivation kinetics, regrowth and synergistic competition in a photocatalytic disinfection system using anatase titanate nanofiber catalyst, Photochem. Photobiol. A – Chem. 214 (2010) 1–9.